

# 1 Ocean liming effects on dissolved organic matter dynamics

2

3 Chiara Santinelli<sup>1</sup>, Silvia Valsecchi<sup>1,2,3</sup>, Simona Retelletti Brogi<sup>1,4</sup>, Giancarlo Bachi<sup>1</sup>, Giovanni  
4 Checcucci<sup>1</sup>, Mirco Guerrazzi<sup>1</sup>, Elisa Camatti<sup>5</sup>, Stefano Caserini<sup>3,6</sup>, Arianna Azzellino<sup>2,3</sup>, Daniela  
5 Basso<sup>3,7</sup>

6

7

1 Consiglio Nazionale delle Ricerche (CNR), Istituto di Biofisica. Via Moruzzi 1, 56124 Pisa (PI), Italia.

8

2 Politecnico di Milano, Dipartimento di Ingegneria Civile ed Ambientale. Piazza Leonardo da Vinci 32, 20133 Milano (MI), Italia.

9

3 Consorzio Nazionale Interuniversitario per le Scienze del Mare (CoNISMa). Piazzale Flaminio 9, 00196 Roma (RM), Italia.

10

4 Istituto di Oceanografia e Geofisica Sperimentale (OGS), Sezione di Oceanografia. Via Piccard 54, 34151 Trieste (TS), Italia.

11

5 Consiglio Nazionale delle Ricerche (CNR), Istituto di Scienze Marine. Arsenale Tesa 104, Castello 2737/F - 30122 Venezia (VE), Italia.

12

6 Università di Parma, Dipartimento di Ingegneria e Architettura. Parco Area delle Scienze 181/A, 43124 Parma (~~P~~PR), Italia.

13

7 Università degli Studi di Milano-Bicocca, Dipartimento di Scienze dell'ambiente e della terra. Piazza della Scienza 4, 20126 Milano (MI), Italia.

14

15

16

*Correspondence to:* Chiara Santinelli (chiara.santinelli@ibf.cnr.it)

17

18 **Abstract.** Ocean liming has gained attention as a potential solution to mitigate climate change by actively removing  
19 carbon dioxide (CO<sub>2</sub>) from the atmosphere. The addition of hydrated lime (~~Ca(OH)<sub>2</sub>~~) into oceanic surface water leads to  
20 an increase in alkalinity, which in turn promotes the uptake and sequestration of atmospheric CO<sub>2</sub>.  
21 Despite the potential of this technique, its effects on the marine ecosystem are still far to be understood, and there is  
22 currently no information on the potential impacts on the concentration and quality of Dissolved Organic Matter (DOM),  
23 that is one of the largest, ~~the~~ most complex and yet the least understood mixture of organic molecules on Earth.  
24 The aim of this study is to provide the first experimental evidence about the potential effects of hydrated lime addition on  
25 DOM dynamics in the oceans, by assessing changes in its concentration and optical properties (absorption and  
26 fluorescence).  
27 ~~The aim of this study is to provide the first experimental evidence about the potential effects of pH peaks, that might be~~  
28 ~~generated by the Ca(OH)<sub>2</sub> dissolution in seawater, on DOM dynamics by assessing changes in its concentration and~~  
29 ~~optical properties (absorption and fluorescence).~~  
30 To investigate the effects of liming on DOM pools with different concentrations and quality, seawater was collected from  
31 two contrasting environments: the oligotrophic Mediterranean Sea (~~MedSea~~), known for its Dissolved Organic Carbon  
32 (DOC) concentration comparable to that observed in the oceans, and the eutrophic Baltic Sea (~~BalSea~~), characterized by  
33 high DOM concentration mostly of terrestrial origin. hydrated limeCa(OH)<sub>2</sub> was added in both waters, to reach a pH of 9  
34 and 10.  
35 Our findings reveal that the addition of hydrated lime has a noticeable effect on DOM dynamics in both the Mediterranean  
36 Sea ~~MedSea~~ and Baltic Sea ~~BalSea~~, determining a reduction in DOC concentration and a change in the optical properties  
37 (absorption and fluorescence) of DOM. These effects, detectable at pH 9, become significant at pH 10 and are more  
38 pronounced in the Mediterranean Sea ~~MedSea~~ than in the Baltic ~~BalSea~~ Sea. These potential short-term effects should be  
39 considered within the context of the physico-chemical properties of seawater and the seasonal variability.

## 40 1 Introduction

41 Oceans are a natural sink for atmospheric CO<sub>2</sub> having the potential to mitigate its increase and therefore the effects of  
42 climate change (Gattuso et al., 2013; Heinze et al., 2015). The massive amount of atmospheric CO<sub>2</sub> absorbed by the  
43 oceans in the last decades (~ 30-40% of anthropogenic emissions), is generating dramatic global-scale changes in seawater  
44 chemistry, such as a decrease in pH, in carbonate concentration and in the ocean buffering capacity (Chikamoto et al.,  
45 2023). Even if the ongoing efforts toward a global reduction of anthropogenic CO<sub>2</sub> emissions should be rapidly intensified,  
46 the available projections highlight the need for additional strategies, such as the development of efficient ocean-based  
47 Negative Emission Technologies (NETs) (Calvin et al., 2023; Royal Society and Royal Academy of Engineering, 2018).  
48 Some NETs are not only capable of removing atmospheric CO<sub>2</sub> and store it as bicarbonate ions into the oceans, but also  
49 of increasing the water pH, restoring ocean buffering capacity to the pre-industrial era (Butenschön et al., 2021; Gore et  
50 al., 2019). One of these NETs is Ocean Alkalinity Enhancement (OAE) (also called Artificial Ocean Alkalinization,  
51 AOA), which relies on the dissolution of alkaline minerals such as hydrated lime (calcium hydroxide, Ca(OH)<sub>2</sub>) into the  
52 oceans (Kheshgi, 1995). Although the exact amount of hydrated lime to be released, as well as its sparging methods, is  
53 still under debate one of the proposals is to discharge highly concentrated slurry (*lime milk*) from large cargo ships, tankers  
54 and/or dedicated vessels. (Caserini et al., (2021) [simulated the pH dynamics within the Modeling studies, simulating the  
55 flow dynamics in the wake of a sparging ship, indicating releasing that the addition of Ca\(OH\)<sub>2</sub> with an initial particle  
56 radius of 45 μm into seawater at a rate of 10 kg s<sup>-1</sup>. The results of their modeling study suggest that in these conditions  
57 can cause a temporary, sharp increase in pH of about 1 unit can be observed at the discharge site, and that the effects  
58 decrease moving far from the discharge site, becoming lower than becoming lower than 0.2 pH units at a distance of,  
59 1400 – 1600 m \(0.8-0.9 nautical miles\), far from the discharge site \(in the hypothesis of a discharge rate of 10 kg s<sup>-1</sup>;](#)  
60 The discharge of alkaline minerals may trigger the inorganic precipitation of calcium carbonate (CaCO<sub>3</sub>), reducing the  
61 efficiency of the CO<sub>2</sub> sink and negatively affecting seawater transparency and photosynthetic rates (González and Ilyina,  
62 2016), with possible consequences for the biogeochemical cycles and the functioning of the marine ecosystem (Camatti  
63 et al., 2024). The side effects of OAE techniques on the marine environment need to be thoroughly investigated before  
64 making any decision on their use. To the best of our knowledge, there is no information on the effects that ocean liming  
65 may have on Dissolved Organic Matter (DOM) and its chromophoric fraction (CDOM, i.e. the light-absorbing fraction  
66 [and FDOM, i.e. its fluorescent fraction](#)). Holding an amount of carbon of 660 billion metric tons and being the most  
67 concentrated dissolved component in the oceans (Hansell et al., 2009), every action that could modify seawater chemistry  
68 is expected to have an impact on this key component of the carbon cycle. DOM represents the main source of energy for  
69 heterotrophic prokaryotes, a change in its concentration and/or quality could therefore have a cascading effect on the  
70 functioning of marine ecosystem.

71 The aim of this study is to provide the first experimental evidence about the potential effects of hydrated lime addition on  
72 DOM dynamics in the oceans, by assessing changes in its concentration and optical properties (absorption and  
73 fluorescence). In order to investigate the impact on DOM pool with different origin and optical properties, seawater was  
74 collected from two highly diverse environments; (1) the oligotrophic Mediterranean Sea (~~MedSea~~), characterized by  
75 Dissolved Organic Carbon (DOC) concentration comparable to those observed in the open oceans, and (2) the eutrophic  
76 Baltic Sea (~~BalSea~~), characterized by high DOC concentration, mostly of terrestrial origin.

77

## 78 2 Materials and methods

79 In order to investigate the effects of ocean liming on DOM dynamics, an ultra-pure  $\text{Ca}(\text{OH})_2$  powder was added to natural  
80 seawater and changes in DOC concentration, absorption and fluorescence of CDOM were followed for 24 hours at the  
81 laboratories of the Biophysics Institute, CNR (Pisa, Italy). ~~Based on the results by Caserini et al. (2021) Caserini et al.~~  
82 ~~(2021), which suggested a sharp increase of 1 unit of pH at the discharge site of a sparging ship, the experiment was~~  
83 ~~carried out at pH 9. Although unlikely under actual conditions of dilution in the open sea, an additional experiment was~~  
84 ~~carried out at pH 10 because this situation may occur in coastal waters (e.g. coastal lagoons, high primary productivity~~  
85 ~~enhanced by eutrophication) (Hinga, 2002) (Hinga, 2002). Based on the results of Caserini et al. (2021) Caserini et al.~~  
86 ~~(2021) The experiments were carried out at pH 9 and 10, based on the results of , which assumes conservative values of~~  
87 ~~lime milk ( $\text{Ca}(\text{OH})_2$  86.5 g/l) discharge rates ( $\leq 25$  kg/s) in the ships' wake.~~  $\text{Ca}(\text{OH})_2$  was provided by UNICALCE  
88 (Sedrina (BG), Italy) and supplied as powder (Tab. S1). Seawater was collected at Marina di Pisa, Tyrrhenian Sea, Italy  
89 (Mediterranean Sea) and in the coastal area surrounding Riga, Latvia (Baltic Sea) (Tab. 1).

90

	Sampling Date	Salinity	pH	DOC ( $\mu\text{M}$ )	$a_{254}$ ( $\text{m}^{-1}$ )	$S_{275-295}$ ( $\text{nm}^{-1}$ )
Med <u>iterranean</u> Sea	Mar-22	38	8.2	$66 \pm 0.5$	1.9	0.024
Balt <u>ic</u> Sea	Apr-22	6	8.1	$364 \pm 3$	24.5	0.021

91 **Table 1: Chemical and physical properties of the Mediterranean Sea and Baltic Sea water used for the**  
92 **experiment.**

93

### 94 2.1 Experimental setup

95 In order to investigate the impact of slaked lime on chemical-physical processes affecting DOM dynamics, seawater was  
96 sterilized by filtration through a 0.2  $\mu\text{m}$  pore size filter (Polycap AS36 filter capsule, Whatman, UK) using a peristaltic  
97 pump (Masterflex<sup>TM</sup> L/S<sup>TM</sup>, Germany). Salinity was measured by using a HI 9033 portable probe (Hanna Instruments,  
98 USA). The experiments were carried out in 2 L acid-washed polycarbonate<sup>®</sup> Nalgene bottles as follows:

99

#### 1. Mediterranean Sea

- a. Treatment: filtered surface seawater enriched with  $\text{Ca}(\text{OH})_2$  powder to reach:
  - pH 9,  $[\text{Ca}(\text{OH})_2]$  0.04 g/L
  - pH 10,  $[\text{Ca}(\text{OH})_2]$  0.25 g/L
- b. Control: filtered surface seawater (pH = 8.2)

100

#### 2. Baltic Sea

- a. Treatment: filtered surface seawater enriched with  $\text{Ca}(\text{OH})_2$  powder to reach
  - pH of 9,  $[\text{Ca}(\text{OH})_2]$  0.01 g/L
  - pH 10,  $[\text{Ca}(\text{OH})_2]$  0.06 g/L
- b. Control: filtered surface seawater (pH = 8.1)

101

102

103

104

105

106

107

108

109 All the experiments were carried out in triplicates and the bottles were stored in the dark and at room temperature ( $22 \pm$   
110  $1 \text{ }^\circ\text{C}$ ). Immediately after the addition of the  $\text{Ca}(\text{OH})_2$  powder, the bottles were gently mixed. Before and after powder  
111 addition and before each sampling time, pH was measured using an edge HI2002-02 pH-meter (Hanna Instruments, USA).  
112 In the treatment at pH 9, the pH slightly decreased by 0.06 (Baltic Sea) and 0.29 (Mediterranean Sea) between 3 and 22  
113 h after the addition (Tab. S2). In the treatment at pH 10, 3 hours after the addition the pH decreased by 0.3 in the  
114 Mediterranean Sea and after 22 hours it decreased by 0.45 in the Mediterranean Sea and 0.26 in the Baltic Sea (Tab. S2).  
115 Subsamples for DOC (40 mL) and CDOM/FDOM (60 mL) analyses were collected before  $\text{Ca}(\text{OH})_2$  addition and 5', 30',  
116 3 h and 22 h after  $\text{Ca}(\text{OH})_2$  addition.  
117 The bottles were gently mixed before subsampling at 5', 30', and 3 h. Since, aAfter 22 hours, carbonate sedimentation  
118 was clearly visible at the bottom of the bottles, after 22 hours, an additional one samples of the supernatant was were  
119 therefore collected before mixing for both DOC and CDOM/FDOM analyses, and an additional sample -was collected  
120 after gently mixing only for DOC analyses, since CDOM/FDOM would have been be strongly affected by the  
121 scattering due to the suspended particles.  
122 Samples for CDOM/FDOM analyses were brought to  $\text{pH } 7.5 \pm 1.0$  with high purity 2 M HCl, to avoid the effect of pH  
123 on DOM absorption and fluorescence and filtered through a PES 0.2  $\mu\text{m}$  pore size syringe filter (Minisart 16534K,  
124 Sartorius, Germany), to avoid the scattering due to the presence of carbonate particles in solution.

125

## 126 2.2 DOC

127 Samples for DOC analysis-analyses were acidified at pH 2 with high purity 2 M HCl. DOC measurements were carried  
128 out with a TOC-L analyzer (Shimadzu, Japan), by high temperature catalytic oxidation following Santinelli et al. (2015).  
129 Samples were sparged for 3 min with  $\text{CO}_2$ -free ultrahigh purity nitrogen to remove inorganic carbon. 150  $\mu\text{L}$  of the sample  
130 were injected into the furnace after a three-fold rinsing with the sample to be analyzed. From 3 to 5 replicate injections  
131 were performed until the analytical error was lower than 1%. A four-point calibration curve was measured using a standard  
132 solution of potassium hydrogen phthalate in the same concentration range as the samples. The system blank was measured  
133 every day at the beginning and the end of the analyses using low-carbon water ( $2\text{-}3 \mu\text{M C}$ ). The instrument performance  
134 was verified daily using the DOC Consensus Reference Material (CRM) (Hansell, 2005) (CRM Batch #20/08-20, nominal  
135 concentration of  $42 \pm 1 \mu\text{M}$ ; measured concentration  $40 \pm 2 \mu\text{M}$ , n of samples 76 -CRM samples analyzed=76).

136

## 137 2.3 CDOM optical properties

### 138 2.3.1 Absorption

139 Absorption spectra were measured between 230 and 700 nm with a UV-Vis spectrophotometer (Mod-7850, Jasco, USA),  
140 using a 10 cm quartz cuvette. The absorption spectrum of Milli-Q water was subtracted from each sample spectrum. The  
141 absorption coefficient at 254 nm ( $a_{254}$ ) and the spectral slope between 275 and 295 nm ( $S_{275-295}$ ) were calculated from the  
142 absorption spectra using the ASFit tool (Omanović et al., 2019).  $a_{254}$  is used to have semi-quantitative information on  
143 CDOM, since primary CDOM absorption is caused by conjugated systems having the absorption peak near 254 nm (Del  
144 Vecchio and Blough, 2004; Weishaar et al., 2003).  $S_{275-295}$  can be related to changes in the average aromaticity and

145 molecular weight of the molecules in the CDOM pool (Helms et al., 2008). ~~The absorption coefficient at 280 nm and 325~~  
146 ~~nm ( $a_{280}$ ,  $a_{325}$ ) and the spectral slope ratio ( $S_r$ , ratio between  $S_{275-295}$  and  $S_{350-400}$ )~~ ~~are also reported for comparison (Tab.~~  
147 ~~S2), being among the most used CDOM indices in the literature.~~

### 148 2.3.2 Fluorescence

149 Fluorescence excitation-emission matrices (EEMs) were recorded with an Aqualog fluorometer (Horiba-Jobin Yvon,  
150 UK), using a 1 cm quartz cuvette. Excitation ranged between 250 and 450 nm at 5 nm increments; emission was recorded  
151 between 212 and 619 nm at 3 nm increments. The EEMs were ~~elaborated-processed~~ using the TreatEEM software  
152 (Omanović et al., 2023). EEMs were corrected for instrumental bias in excitation and emission, and Rayleigh and Raman  
153 scatter peaks were removed using the monotone cubic interpolation (shape-preserving). EEMs were normalized to the  
154 water Raman signal, dividing the fluorescence by the integrated Raman band of Milli-Q water ( $\lambda_{ex} = 350$  nm,  $\lambda_{em} = 371$ -  
155 428 nm; Lawaetz and Stedmon, 2009) measured on the same day of the analyses. The fluorescence intensity is therefore  
156 reported as equivalent to water Raman Units (R.U.).

157 Parallel factor analysis (PARAFAC) was separately applied to the Mediterranean Sea (~~number of EEMs: 63~~) and Baltic  
158 Sea (~~number of EEMs: 50~~) samples (number of EEMs: 45 for each experiment), using the decomposition routines of the  
159 EEMs toolbox for MATLAB software (drEEM) (Murphy et al., 2013). The PARAFAC validated a 3-component model  
160 for both the Mediterranean Sea and the Baltic Sea (Fig. S1 and S2). OpenFluor, an online database of environmental  
161 fluorescence spectra, was used as a validation tool to characterize the three components (Tab. S2-S3 and S3S4). OpenFluor  
162 compares excitation and emission spectra of the validated components with all the components present in the database  
163 and allows comparing the spectra using the Tucker Congruence Coefficient (TCC; Murphy et al. (2014)).

164

### 165 2.4 Statistical analyses

166 For all parameters, differences were tested using the Kruskal-Wallis nonparametric test and were considered significant  
167 at the threshold of  $p < 0.05$ . All statistical analyses were performed using OriginPro version 9 (OriginLab, USA).

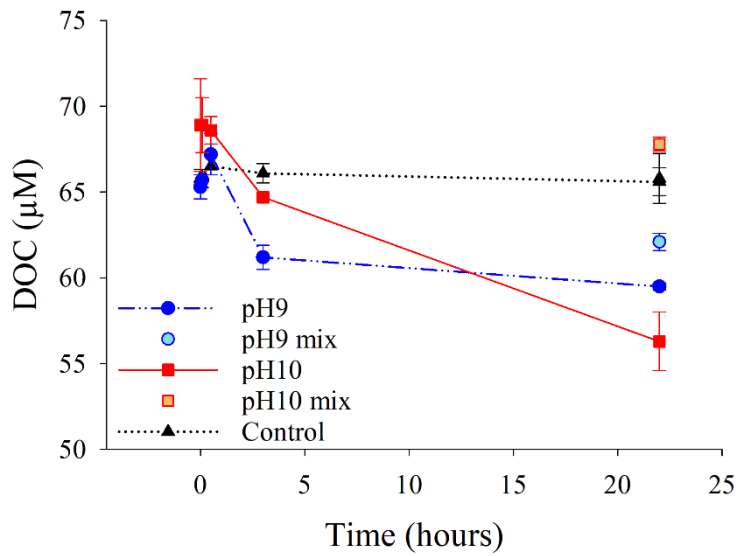
168

## 169 3. Results

### 170 3.1 Mediterranean Sea

#### 171 3.1.1 DOC

172 In the ~~MedSea~~ Mediterranean Sea, ~~DOC concentration was  $67 \pm 2 \mu\text{M}$ .~~ ~~Three hours after  $\text{Ca}(\text{OH})_2$  addition, a  $4 \mu\text{M}$  (6%)~~  
173 ~~DOC decrease was observed in both treatments (Fig. 1, Tab. S2).~~ A further decrease was observed in the supernatant of  
174 the unmixed sample 22 h after the addition, with DOC reaching  $59.5 \pm 0.2 \mu\text{M}$  (~~429%~~ decrease) at pH 9 and  $56.3 \pm 1.7$   
175  $\mu\text{M}$  (~~186%~~ decrease) at pH 10 (Tab. S2). It is noteworthy that such a decline was only observed in the unmixed samples,  
176 whereas no significant change was observed in the mixed samples 22 h after the addition (Fig. 1, ~~and Tab. S2).~~



177

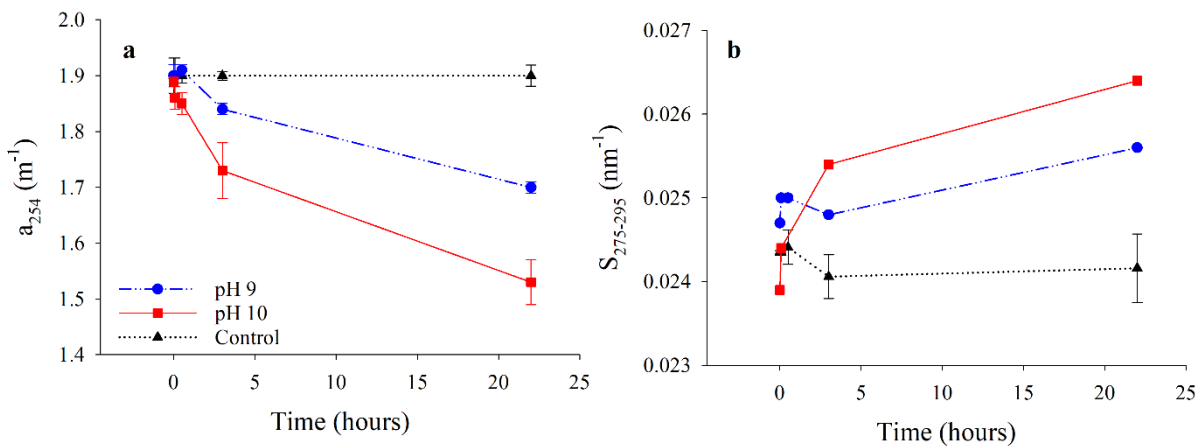
178 **Figure 1: Trend of DOC concentration in the MedSeaMediterranean Sea treatments at pH 9 and 10, and in the**  
 179 **control. Error bars refer to the standard deviation among the 3 replicates. Please, note that for some samples the**  
 180 **error bars are smaller than the symbols and therefore not visible.**

181

182

### 183 3.1.2 CDOM Absorption

184 A slight decrease in  $a_{254}$  was observed 3 hours after  $\text{Ca}(\text{OH})_2$  addition at both pH (9 and 10). Interestingly, 22 h after the  
 185 addition, in the supernatant of unmixed bottles, a marked decrease of  $0.2 \text{ m}^{-1}$  (44.10%) and  $0.4 \text{ m}^{-1}$  (20.19%) was observed  
 186 (Fig. 2a, Tab. S2) together with an increase in  $S_{275-295}$  from  $0.02474 \text{ nm}^{-1}$  to  $0.0256 \text{ nm}^{-1}$  (64%) and from 0.0239 to  $0.0264$   
 187  $\text{nm}^{-1}$  (10%) at pH 9 and 10, respectively (Fig. 2b, Tab. S2). Mixed samples were not collected for CDOM analyses, since  
 188 scattering due to the particles would have affected the results.



189

190 **Figure 2: Trend of  $a_{254}$  (a) and  $S_{275-295}$  (b) in the MedSeaMediterranean Sea treatments at pH 9 and 10, and in the**  
 191 **control. Error bars refer to the standard deviation among the 3 replicates. Please, note that for some samples the**  
 192 **error bars are smaller than the symbols and therefore not visible.**

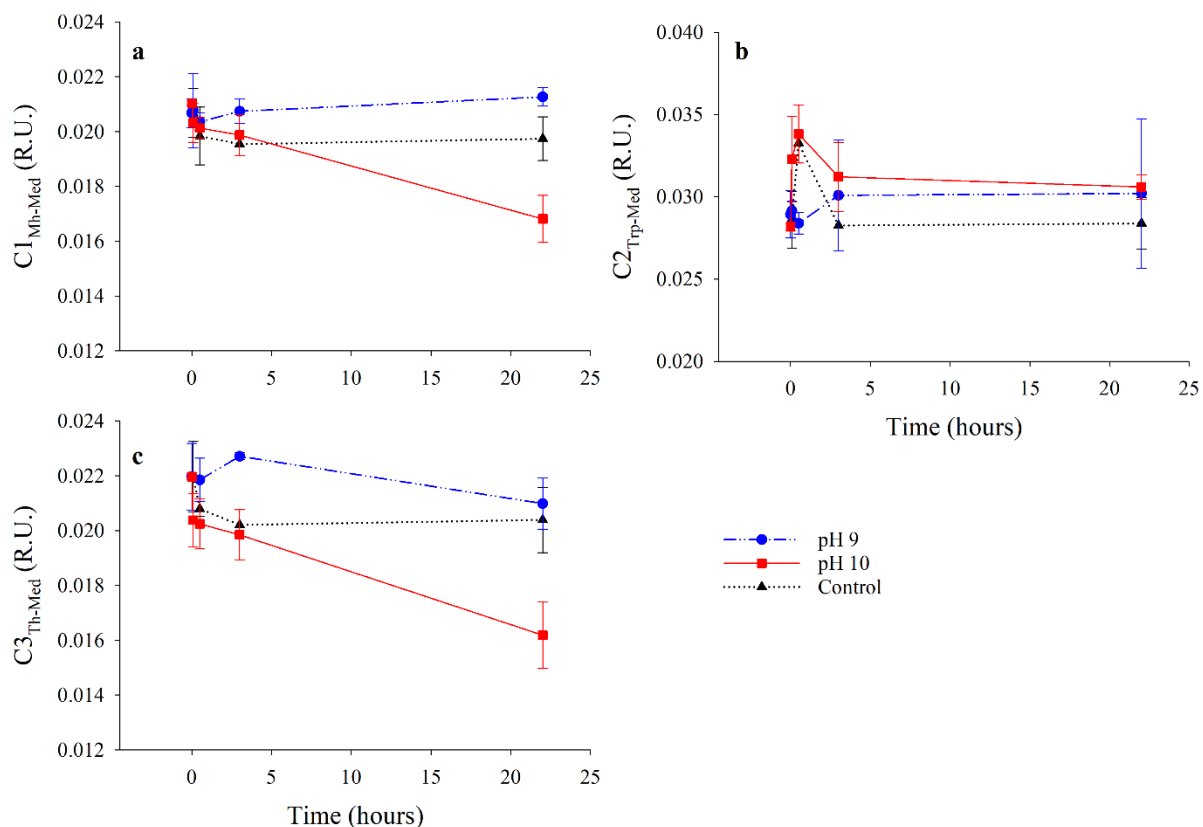
193

194

### 195 3.1.3 FDOM fluorescence

196 The PARAFAC validated a ~~3-component~~3-component model for the ~~MedSea~~Mediterranean Sea EEMs (Fig. S1, Tab.  
197 ~~S2S3~~). Component 1 ( $\lambda_{Ex}/\lambda_{Em}$ : 315/409 nm, Fig. S1a) shows spectroscopic characteristics similar to Coble's peak M  
198 ( $\lambda_{Ex}/\lambda_{Em}$ : 312/[380]420; Coble (1996)). The comparison with similar components in the OpenFluor database (matches  
199 with a TCC > 0.95) allowed to characterize it as marine humic-like (C1<sub>Mh-Med</sub>). Component 2 ( $\lambda_{Ex}/\lambda_{Em}$ : 275/331 nm, Fig.  
200 S1b) shows spectroscopic characteristics similar to Coble's peak T ( $\lambda_{Ex}/\lambda_{Em}$ : 275/340 nm; Coble (1996)). The comparison  
201 with similar components in the OpenFluor database (matches with a TCC > 0.95) allowed to characterize it as  
202 ~~T~~tryptophan-like (C2<sub>Trp-Med</sub>). Component 3 ( $\lambda_{Ex}/\lambda_{Em}$ : 260/[380]456 nm, Fig. S1c) shows spectroscopic characteristics  
203 similar to Coble's peaks C and A ( $\lambda_{Ex}/\lambda_{Em}$ : 350/451 and 245/451 nm, respectively; Coble (1996)). The comparison with  
204 similar components in the OpenFluor database (matches with a TCC > 0.95) allowed to characterize it as terrestrial humic-  
205 like (C3<sub>Th-Med</sub>).

206 C1<sub>Mh-Med</sub> did not show significant changes over the incubation time at pH 9 and in the control (Fig. 3a, Tab. S5). At pH  
207 10, a decrease of 0.004 R.U. (~~2049~~%) was observed 22 h after the addition. C2<sub>Trp-Med</sub> did not show significant changes  
208 during the incubation, neither in the treatments nor in the control (Fig. 3b, Tab. S5). C3<sub>Th-Med</sub> showed variations only at  
209 pH 10 (Fig. 3c, Tab. S5), with a slight decrease 3 hours after the addition, and a significant decrease of 0.006 R.U. (26%)  
210 at the end of the incubation (22 h).



211



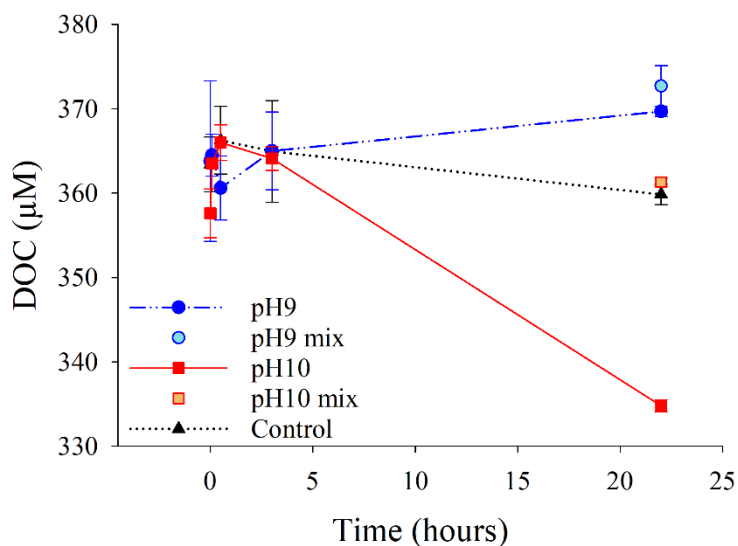
212 **Figure 3: Trend of the fluorescent intensity of C1<sub>Mh-Med</sub> (a), C2<sub>Trp-Med</sub> (b) and C3<sub>Th-Med</sub> (c) in the**  
 213 **MedSeaMediterranean Sea** treatments at pH 9 and 10, and in the control. Error bars refer to the standard  
 214 deviation among the 3 replicates.

215

## 216 3.2 Baltic Sea (BalSea)

### 217 3.2.1 DOC

218 In the Baltic Sea, DOC concentration was  $362 \pm 3 \mu\text{M}$ . No significant change was observed 3 hours after  $\text{Ca}(\text{OH})_2$   
 219 addition in both treatments (pH 9 and 10) (Fig. 4, Tab. S2). At the end of the experiment (22 h), DOC decreased by ~~27~~  
 220 23  $\mu\text{M}$  (67 %) at pH 10, whereas no significant change was observed at pH 9. It is noteworthy that DOC showed  
 221 significant differences between the mixed and unmixed samples at pH 10, whereas in the mixed samples DOC was similar  
 222 to the control (Fig. 4, Tab. S2).



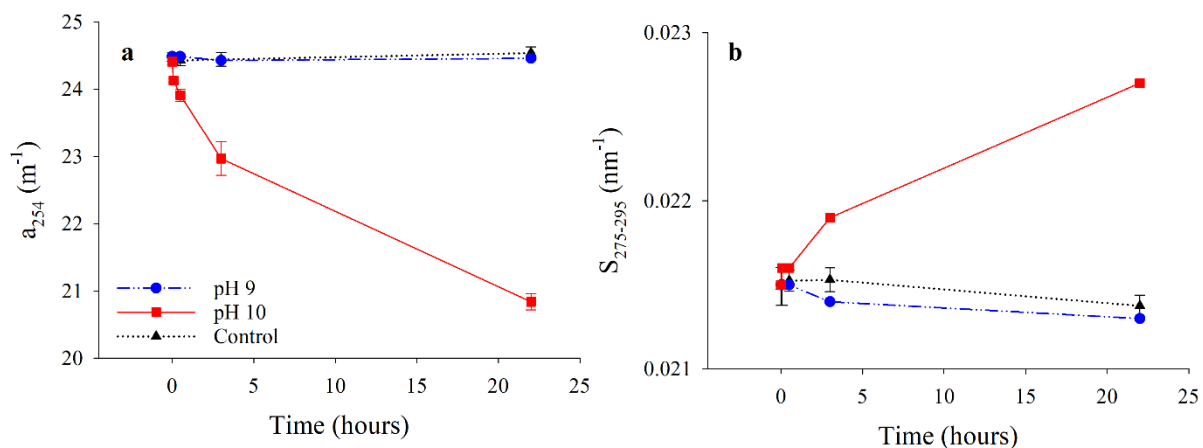
223

224 **Figure 4: Trend of DOC concentration in the Baltic Sea treatments at pH 9 and 10 and in the control. Error bars**  
 225 **refer to the standard deviation among the 3 replicates. Please, note that for some samples the error bars are**  
 226 **smaller than the symbols and therefore not visible.**

227

### 228 3.2.2 CDOM absorption

229 Twenty-two hours after the addition of  $\text{Ca}(\text{OH})_2$ ,  $a_{254}$  decreased by  $0.03 \text{ m}^{-1}$  (0.13%), and  $3.76 \text{ m}^{-1}$  (15%) at pH 9 and pH  
 230 10, respectively (Fig. 5a).  $S_{275-295}$  increased from  $0.0215 \text{ nm}^{-1}$  to  $0.023-0.027 \text{ nm}^{-1}$  (6%) at pH 10, whereas no significant  
 231 change was observed at pH 9 (Fig. 5b). The change in CDOM is therefore visible only at pH 10 (Fig. 5)



232

233 **Figure 5: Trend of  $a_{254}$  (a) and  $S_{275-295}$  (b) in the Baltic Sea treatments at pH 9 and 10, and in the control. Error**  
 234 **bars refer to the standard deviation among the 3 replicates. Please, note that for some samples the error bars are**  
 235 **smaller than the symbols and therefore not visible.**

236

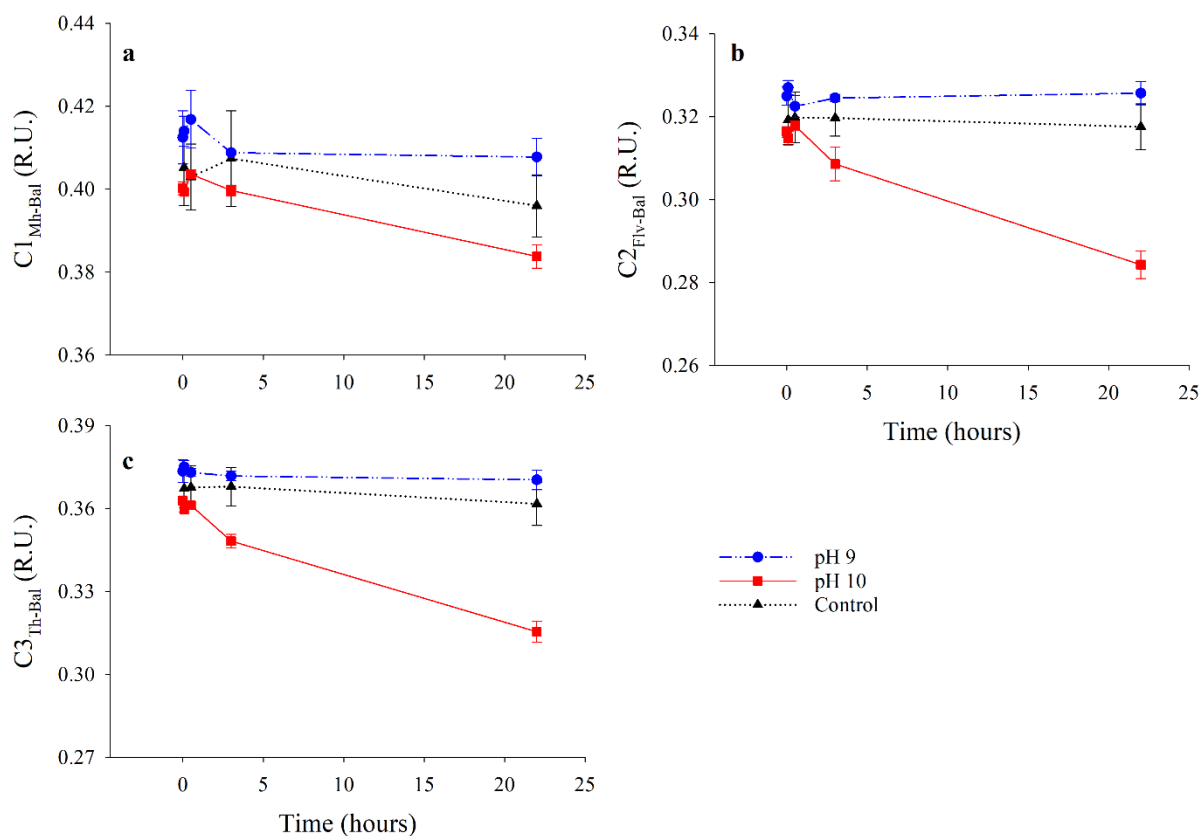
237

### 238 3.2.3 FDOM fluorescence

239 The PARAFAC validated a 3-component model for the Baltic Sea EEMs experiment (Fig. S2, Tab. S3). Component 1  
 240 ( $\lambda_{Ex}/\lambda_{Em}$ : 290/400 nm, Fig. S2) shows spectroscopic characteristics similar to Coble's peak M ( $\lambda_{Ex}/\lambda_{Em}$ : 312/[380]420;  
 241 Coble (1996)). The comparison with similar components in the OpenFluor database (matches with a TCC > 0.95) allowed  
 242 to characterize it as marine humic-like ( $C1_{Mh-Bal}$ ). Component 2 ( $\lambda_{Ex}/\lambda_{Em}$ : 330/452 nm, Fig. S2) shows spectroscopic  
 243 characteristics similar to Coble's peak C ( $\lambda_{Ex}/\lambda_{Em}$ : 350/451; Coble (1996)). The comparison with similar components in  
 244 the OpenFluor database (matches with a TCC > 0.95) allowed to characterize it as Fulvic-like ( $C2_{Flv-Bal}$ ). Component 3  
 245 ( $\lambda_{Ex}/\lambda_{Em}$ : 280/485 nm, Fig. S2) shows spectroscopic characteristics similar to Coble's peak A ( $\lambda_{Ex}/\lambda_{Em}$ : 260/[380]460 nm;  
 246 Coble (1996)). The comparison with similar components in the OpenFluor database (matches with a TCC > 0.95) allowed  
 247 to characterize it as Terrestrial humic-like ( $C3_{Th-Bal}$ ).

248  $C1_{Mh-Bal}$  did not show significant changes during the incubation neither in the treatments nor in the control (Fig. 6a, Tab.  
 249 S5).  $C2_{Flv-Bal}$  did not show significant changes during the incubation at pH 9 and in the control, whereas a decrease of  
 250 0.03 R.U. (9-10%) was observed at pH 10 ~~between 30 minutes and after~~ 22 hours (Fig. 6b, Tab. S5).  $C3_{Th-Bal}$  did not show  
 251 significant changes during the incubation at pH 9 and in the control, whereas a decrease of 0.04-05 R.U. (13-14%) was  
 252 observed at pH 10 ~~between 30 minutes and after~~ 22 hours (Fig. 6c, Tab. S5).

253



254

255 **Figure 6: Trend of the fluorescent intensity of  $C1_{Mh-Bal}$  (a),  $C2_{Flv-Bal}$  (b) and  $C3_{Th-Bal}$  (c) in the Baltic Sea**  
 256 **treatments at pH 9 and 10, and in the control. Error bars refer to the standard deviation among the 3 replicates.**  
 257 **Please, note that for some samples the error bars are smaller than the symbols and therefore not visible.**

258

259

## 260 4 Discussion

261 Even if OAE using alkaline minerals is considered a promising tool to mitigate climate change through the sequestration  
 262 and storage of atmospheric  $CO_2$  into the ocean (DOSI, 2022), its impact on the marine ecosystem is still far to be  
 263 understood. To the best of our knowledge, this is the first study investigating the potential effects of OAE by hydrated  
 264 lime addition on DOM dynamics, with particular regard to DOC concentration and CDOM optical properties. Given the  
 265 crucial role that DOM plays in the marine ecosystem, any impact on its dynamics is expected to affect the water quality  
 266 and ecosystem functioning through a cascading effect on the microbial loop and the microbial food web.

267

### 268 4.1 Liming impact on DOM dynamics

269 Our data show the potential effects of hydrated lime addition ~~OAE~~ on DOM dynamics determining a decrease in DOC  
 270 concentration (Fig. 1 and 4) and a change in the optical properties of CDOM (Fig. 2, 3, 5 and 6). The decrease in  $a_{254}$ , the  
 271 increase in  $S_{275-295}$  (Fig. 2 and 5) and the decrease in humic-like fluorescence (Fig. 3 and 6) indicate a change in DOM

272 quality with a shift towards molecules with lower average molecular weight and aromaticity degree. These effects are  
273 already visible at pH 9, but becomes relevant at pH 10. Different hypotheses can explain our results:

- 274 1) DOM reacts with  $\text{Ca}(\text{OH})_2$  and the largest and most aromatic molecules are oxidized to  $\text{CO}_2$ ;
- 275 2) the largest and most aromatic molecules adsorb onto primary and secondary carbonate precipitates, that form  
276 following the  $\text{Ca}(\text{OH})_2$  addition, and sink;
- 277 3) the largest and most aromatic molecules aggregate forming polymer gels or large colloidal material and sink.

278 Interestingly, a significant decrease in DOC concentration was observed only in the unmixed samples at the end of the  
279 experiment (22 h after the addition, Fig. 1 and 4), DOC oxidation to  $\text{CO}_2$  by reaction with  $\text{Ca}(\text{OH})_2$  (hypothesis 1) can  
280 therefore be ruled out as a possible removal mechanism. The other 2 hypotheses remain plausible and are supported by  
281 the available literature (Conzonno and Cirelli, 1995; Kaushal et al., 2020; Leenheer and Reddy, 2008; Pace et al., 2012).  
282 In lake waters, DOM was observed to adsorb onto carbonate particles and co-precipitate with them; the use of  $\text{CaCO}_3$   
283 precipitation was indeed suggested as an efficient technique for DOM removal during drinking water treatment processes  
284 (Leenheer and Reddy, 2008). The mechanism of DOM co-precipitation and/or physical incorporation into  $\text{CaCO}_3$  is due  
285 to the formation of insoluble calcium. This hypothesis is further supported by the observation of  $\text{CaCO}_3$  precipitation  
286 following the dissolution of hydrated lime, that was enhanced by the occurrence of nucleation surfaces as particles or  
287 solid mineral phases in the solution (Moras et al., 2021).

288 In freshwater ponds, a high affinity of high molecular weight molecules to adsorb onto particles like  $\text{CaCO}_3$  was observed  
289 by Conzonno and Cirelli (1995) together with a preferential removal of high molecular weight humic substances during  
290  $\text{CaCO}_3$  crystals formation. Since humic acids have important environmental functions in controlling the pH and the  
291 bioavailability of dissolved metals (Baalousha et al., 2006), their removal may trigger a cascade effect with possible  
292 impacts on water quality. Past studies showed that pH per se can affect DOM dynamics as DOM can undergo a fast  
293 transition from dissolved to polymer gels (Chin et al., 1998) or large colloidal material (Pace et al., 2012) when pH  
294 switches toward more basic values ( $\text{pH} > 8$  for seawater).

295 Among the ~~three~~ 3 hypotheses mentioned above, the ~~observed~~ decrease in  $a_{254}$ , observed in our experiments, supports the  
296 hypothesis 2, suggesting that, following the addition of  $\text{Ca}(\text{OH})_2$ , the largest and most aromatic dissolved organic  
297 molecules adsorb to primary and secondary mineral particles and sink. This hypothesis is further supported by the high  
298 removal of the terrestrial components observed in both the Mediterranean Sea ( $C_{3\text{Th Med}}$ , -26%) and the Baltic Sea ( $C_{3\text{Th}}$   
299  $B_{\text{Bal}}$ , -13%). This observation agrees with the results of Kaushal et al., (2020) which reported a higher incorporation of the  
300 terrestrial humic substances into abiogenically precipitated aragonite, then transferred within coral skeletons, with respect  
301 to marine humic substances.

302  
303

#### 304 4.2 Different effects on Mediterranean and Baltic waters

305 The ~~MedSea~~ Mediterranean Sea and the ~~BalSea~~ Baltic Sea are basins with different biogeochemical characteristics (Tab.  
306 1). Our results show that DOC concentration (Fig. 1 and 4) and  $a_{254}$  (Fig. 2 and 5) are 6 and 13 times higher in the  
307 ~~BalSea~~ Baltic Sea than in the ~~MedSea~~ Mediterranean Sea (Tab. 1),— these data are consistent with previous studies

308 (Hoikkala et al., 2015; Santinelli, 2015; Santinelli et al., 2010). The lower  $S_{275-295}$  (Tab. 1) and the different FDOM  
309 composition (Fig. S1 and S2) indicate a higher percentage of terrestrial DOM in the Baltic Sea than in the  
310 Mediterranean Sea, as previously reported by Deutsch et al. (2012) and Hoikkala et al. (2015). Indeed, in the Baltic Sea  
311 Sea, PARAFAC allowed to characterize humic-like and fulvic-like components but not protein-like ones (Fig. S2, Tab.  
312 S34), differently ~~from in the Mediterranean Sea where~~ the protein-like component was identified (Fig. S1, Tab.  
313 S32). Protein-like compounds are usually related to in-situ production, whereas fulvic-like substances mostly have a  
314 terrestrial origin. The predominance of terrestrial DOM in the Baltic Sea is due to the high freshwater input from  
315 the wide catchment area (~ 4 times as large as the sea itself), and the low seawater input from the North Sea. The  
316 Baltic Sea is also characterized by a peculiar carbonate system (Kuliński et al., 2017), exhibiting a wider range of  
317 total alkalinity (and pH) compared to the oceans. In particular, the Gulf of Riga, where the water for our experiment was  
318 collected, is characterized by a higher total alkalinity and a higher pH with respect to the rest of the Baltic Sea  
319 (Beldowski et al., 2010; Kuliński et al., 2017).

320 In our experiments, we observed a different impact of  $\text{Ca}(\text{OH})_2$  addition in the Mediterranean Sea and  
321 Baltic Sea water. In the Mediterranean Sea, a DOC decrease of 8.6 and 13.4  $\mu\text{M}$  was recorded at pH 9 and  
322 10, respectively (Tab. S2), indicating a net removal up to 46.18% of the initial DOC (Fig. 1, Tab. S2). In the Baltic Sea  
323 Sea, the maximum removal observed was 86% at pH 10, whereas no effect was recorded at pH 9 (Fig. 4).

324 Even if the salinity, being markedly lower in the Baltic Sea than in the Mediterranean Sea, is probably the  
325 main driver of the ~~lower precipitation of  $\text{CaCO}_3$ , and consequently of the~~ less pronounced effects on DOM dynamic, it  
326 cannot be excluded that the peculiar carbonate system combined with the different concentration and quality of DOM  
327 may have influenced the lower removal rates observed in our experiment. The influence of water chemistry is already  
328 evident by the 4-times lower amount of  $\text{Ca}(\text{OH})_2$  needed to reach pH 9 and 10 in the Baltic Sea than in the  
329 Mediterranean Sea. Since  $\text{CaCO}_3$  precipitation can be one of the main mechanisms explaining our results, the  
330 lower amount of  $\text{Ca}(\text{OH})_2$  added in the Baltic Sea can explain the lower decrease of DOC observed in this basin  
331 than in the Mediterranean Sea. ~~At pH 10, the overall DOC removed in the Baltic Sea is larger (27  $\mu\text{M}$ ) than in~~  
332 ~~the Mediterranean Sea (11  $\mu\text{M}$ ), despite the lower  $\text{Ca}(\text{OH})_2$  added. This suggests a removal of 450  $\mu\text{mol}$  of DOC per~~  
333 ~~gram of  $\text{Ca}(\text{OH})_2$  added in the Baltic Sea, and 44  $\mu\text{mol}$  of DOC per gram of  $\text{Ca}(\text{OH})_2$  added in the Mediterranean Sea.~~  
334 ~~This observation can be explained by the predominance of terrestrial DOM in the Baltic Sea which was suggested to be~~  
335 ~~preferentially removed during abiogenic precipitation of aragonite with respect to marine DOM~~ (Kaushal et al., 2020).

336 It is noteworthy that DOM in the Mediterranean Sea and in the oceans shows a clear seasonal cycle, mostly  
337 attributed to the changes in temperature, water stratification and biological activity, affecting DOM concentration, optical  
338 properties and stoichiometry (Carlson and Hansell, 2015; Santinelli, 2015; Santinelli et al., 2013). Seasonality strongly  
339 affects DOM dynamics also in the Baltic Sea with prevalent allochthonous sources in winter and in-situ production  
340 by phytoplankton in spring (Hoikkala et al., 2012; Seidel et al., 2017). ~~Our results, combined with the observed seasonality~~  
341 ~~in DOM dynamics, stress~~ ~~By integrating these observations with the outcomes of our study, it becomes evident~~ that any  
342 ~~hypothesis plans for~~ liming-based OAE should ~~not only account for the physico-chemical properties of each basin but~~  
343 also ~~take into consideration the~~ seasonal variability.

344

### 345 4.3 Changed DOM dynamics: implication for the marine ecosystems

346 Our results suggest that CaCO<sub>3</sub> precipitation is the main driver for the sequestration of DOM from the water column. The  
347 sinking of the largest and most complex fraction of DOM to the deep oceans could lead to different scenarios.

348 1. If the exported [DOC-DOM](#) is labile (i.e. it is available to microbial removal on the short temporal scale), its export  
349 would determine:

- 350 • A depletion of the energy available for heterotrophic prokaryotes in the surface layer, determining a  
351 malfunctioning of the microbial loop that could impact the energy transfer to the higher trophic levels. This  
352 process could be further enhanced if the primary production is limited by the reduced water transparency  
353 due to carbonate formation.
- 354 • The export of energy to the deepest layer (below the carbon compensation depth, CCD), leading to an  
355 increased bacterial production, in response to the labile DOM released due to the CaCO<sub>3</sub> dissolution.

356 2. If the exported [DOC-DOM](#) is refractory (i.e. it is not available to microbial removal on the short temporal scale), it  
357 will contribute to C sequestration in the deep waters.

358 Our results indicate the preferential removal of the humic-like fractions by CaCO<sub>3</sub> precipitation. Humic-like substances  
359 are considered to constitute the less labile fraction of DOM (Bachi et al., 2023; Zigah et al., 2017). ~~(Zigah et al., 2017;~~  
360 ~~Bachi et al., 2023), supporting C sequestration in the deep waters (hypothesis 2) and a change in the lability of DOM in~~  
361 ~~the surface waters, with an increase in the percentage of the labile fraction after CaCO<sub>3</sub> formation. Even if the lability of~~  
362 ~~DOM is a very complex process, depending on a large number of variables (Dittmar et al., 2021), the change in the lability~~  
363 ~~of DOM could be tested in incubation experiments with natural microbial communities collected in the same area as the~~  
364 ~~water used for the experiment. The water for the experiments was filtered through a 0.2 µm filter and it was therefore~~  
365 ~~considered sterile, in order to investigate the potential removal of DOM by microbes, we could inoculate the natural~~  
366 ~~microbial community adding a 10% of unfiltered water from the same site. In order to avoid artefacts from direct pH~~  
367 ~~impacts on the microbial community, before the inoculum the pH should be brought to natural pH by adding HCl.~~  
368 ~~It should also be taken into consideration that the adsorption of DOM onto CaCO<sub>3</sub> particles, itself might reduce the~~  
369 ~~bioavailability, regardless of the inherent properties of the DOM. This process would increase the carbon sequestration~~  
370 ~~into the deep waters, but it would reduce the energy available for the marine ecosystems. ;~~

371

### 372 5. Conclusions

373 This study reports the first evidence of the potential effects of OAE on DOM dynamics in two contrasting environments:  
374 the oligotrophic [MedSeaMediterranean Sea](#), known for its low DOC concentration, and the eutrophic [Baltic Sea](#),  
375 characterized by high DOM concentration mostly of terrestrial origin. Our findings suggest that ocean alkalization by  
376 Ca(OH)<sub>2</sub> sparging may alter DOM dynamics and, consequently, have a potential impact on the entire marine ecosystem.  
377 To mitigate these effects, it is crucial to reduce the duration and intensity of pH spikes, ensuring they remain below the  
378 safety threshold of pH 9. We stress the need to take into consideration the physico-chemical properties (e.g. salinity, pH,

379 DOM concentration and quality) of the basin and the season, to efficiently manage ocean liming and mitigate the potential  
380 impacts of ocean alkalization on DOM pool.

381 Although the experimental conditions used in this study were more severe than actual liming practices, where the release  
382 of  $\text{Ca}(\text{OH})_2$  in the ship's wake undergoes rapid dilution that significantly reduces pH changes, our results provide new  
383 insights into the possible impacts due to physico-chemical processes.

384 It is important to highlight that the experiments in this study were conducted using sterilized seawater, thus excluding the  
385 potential interplay of biological processes on DOM dynamics. To gain a more comprehensive understanding of possible  
386 OAE impacts, future research should address the influence of biological processes, as well as factors like dilution rates,  
387 water mixing, and realistic durations and severities of pH peaks. Scaling up the experimental setup to mesocosms would  
388 allow for repeated additions and longer observation periods, enabling a more accurate representation of real-world  
389 conditions.

390

#### 391 **Author contribution**

392 Conceptualization by CS, DB and AA. CS designed and supervised the experiments and SV, RBS, GB, GC, MG carried them out.

393 Funding acquisition by SC and AA. CS prepared the manuscript with contributions from all co-authors.

394

#### 395 **Competing interests**

396 The authors declare that they have no conflict of interest.

397

#### 398 **Acknowledgements**

399 The current study has received funding from European Lime Association (EuLA) through a research contract established with CoNISM  
400 (National Inter-University Consortium for Marine Sciences) in Italy. We warmly thank Roberto Moreschi and Dario Ravasio  
401 (UNICALCE Sedrina) for kindly sending the samples of Ca-hydroxide used for our experiments. We thank Giovanni Cappello  
402 (Limenet) and Agija Bistere (Hyrogas) for sampling and sending to Pisa the Baltic [Sea](#) seawater. The authors are grateful to Marco  
403 Carloni and Valtere Evangelista for their support in sampling of [MedSeaMediterranean Sea](#) water and CDOM/FDOM analyses and to  
404 Rosanna Cascone, Rosanna Claps and Claudia Neri, (IBF-CNR, Italy) for the assistance in the financial management. The authors wish  
405 to thank Aurela Shitza and Marlena Wissel from EuLA for their valuable feedback and helpful suggestions which greatly contributed to  
406 the overall improvement of this paper.  
407

408 **References**

- 409 Baalousha, M., Kammer, F. V. D., Motelica-Heino, M., Hilal, H. S., and Le Coustumer, P.: Size  
410 fractionation and characterization of natural colloids by flow-field flow fractionation coupled to multi-angle  
411 laser light scattering, *J Chromatogr A*, 1104, 272–281, <https://doi.org/10.1016/j.chroma.2005.11.095>, 2006.
- 412 Bachi, G., Morelli, E., Gonnelli, M., Balestra, C., Casotti, R., Evangelista, V., Repeta, D. J., and Santinelli,  
413 C.: Fluorescent properties of marine phytoplankton exudates and lability to marine heterotrophic prokaryotes  
414 degradation, *Limnol Oceanogr*, 68, 982–1000, <https://doi.org/10.1002/lno.12325>, 2023.
- 415 Beldowski, J., Löffler, A., Schneider, B., and Joensuu, L.: Distribution and biogeochemical control of total  
416 CO<sub>2</sub> and total alkalinity in the Baltic Sea, *Journal of Marine Systems*, 81, 252–259,  
417 <https://doi.org/10.1016/j.jmarsys.2009.12.020>, 2010.
- 418 Butenschön, M., Lovato, T., Masina, S., Caserini, S., and Grosso, M.: Alkalinization Scenarios in the  
419 Mediterranean Sea for Efficient Removal of Atmospheric CO<sub>2</sub> and the Mitigation of Ocean Acidification,  
420 *Frontiers in Climate*, 3, 614537, <https://doi.org/10.3389/fclim.2021.614537>, 2021.
- 421 Calvin, K., Dasgupta, D., Krinner, G., Mukherji, A., Thorne, P. W., Trisos, C., Romero, J., Aldunce, P.,  
422 Barrett, K., Blanco, G., Cheung, W. W. L., Connors, S., Denton, F., Diongue-Niang, A., Dodman, D.,  
423 Garschagen, M., Geden, O., Hayward, B., Jones, C., Jotzo, F., Krug, T., Lasco, R., Lee, Y.-Y., Masson-  
424 Delmotte, V., Meinshausen, M., Mintenbeck, K., Mokssit, A., Otto, F. E. L., Pathak, M., Pirani, A.,  
425 Poloczanska, E., Pörtner, H.-O., Revi, A., Roberts, D. C., Roy, J., Ruane, A. C., Skea, J., Shukla, P. R.,  
426 Slade, R., Slangen, A., Sokona, Y., Sörensson, A. A., Tignor, M., van Vuuren, D., Wei, Y.-M., Winkler, H.,  
427 Zhai, P., Zommers, Z., Hourcade, J.-C., Johnson, F. X., Pachauri, S., Simpson, N. P., Singh, C., Thomas, A.,  
428 Totin, E., Alegría, A., Armour, K., Bednar-Friedl, B., Blok, K., Cissé, G., Dentener, F., Eriksen, S., Fischer,  
429 E., Garner, G., Guivarch, C., Haasnoot, M., Hansen, G., Hauser, M., Hawkins, E., Hermans, T., Kopp, R.,  
430 Leprince-Ringuet, N., Lewis, J., Ley, D., Ludden, C., Niamir, L., Nicholls, Z., Some, S., Szopa, S., Trewin,  
431 B., van der Wijst, K.-I., Winter, G., Witting, M., Birt, A., and Ha, M.: IPCC, 2023: Climate Change 2023:  
432 Synthesis Report. Contribution of Working Groups I, II and III to the Sixth Assessment Report of the  
433 Intergovernmental Panel on Climate Change [Core Writing Team, H. Lee and J. Romero (eds.)]. IPCC,  
434 Geneva, Switzerland., <https://doi.org/10.59327/IPCC/AR6-9789291691647>, 2023.
- 435 Camatti, E., Valsecchi, S., Caserini, S., Barbaccia, E., Santinelli, C., Basso, D., and Azzellino, A.: Short-term  
436 impact assessment of ocean liming: A copepod exposure test, *Mar Pollut Bull*, 198, 115833,  
437 <https://doi.org/10.1016/j.marpolbul.2023.115833>, 2024.
- 438 Carlson, C. A. and Hansell, D. A.: DOM Sources, Sinks, Reactivity, and Budgets, in: *Biogeochemistry of*  
439 *Marine Dissolved Organic Matter*, 65–126, <https://doi.org/10.1016/B978-0-12-405940-5.00003-0>, 2015.
- 440 Caserini, S., Pagano, D., Campo, F., Abbà, A., De Marco, S., Righi, D., Renforth, P., and Grosso, M.:  
441 Potential of Maritime Transport for Ocean Liming and Atmospheric CO<sub>2</sub> Removal, *Frontiers in Climate*, 3,  
442 575900, <https://doi.org/10.3389/fclim.2021.575900>, 2021.
- 443 Chikamoto, M. O., DiNezio, P., and Lovenduski, N.: Long-Term Slowdown of Ocean Carbon Uptake by  
444 Alkalinity Dynamics, *Geophys Res Lett*, 50, <https://doi.org/10.1029/2022GL101954>, 2023.
- 445 Chin, W.-C., Orellana, M. V., and Verdugo, P.: Spontaneous assembly of marine dissolved organic matter  
446 into polymer gels, *Nature*, 391, 568–572, <https://doi.org/10.1038/35345>, 1998.
- 447 Coble, P.: Characterization of marine and terrestrial DOM in seawater using excitation-emission matrix  
448 spectroscopy, *Mar Chem*, 51, 325–346, 1996.
- 449 Conzonno, V. H. and Cirelli, A. F.: Dissolved organic matter in Chascomus Pond (Argentina). Influence of  
450 calcium carbonate on humic acid concentration, *Hydrobiologia*, 297, 55–59,  
451 <https://doi.org/10.1007/BF00033501>, 1995.



452 Del Vecchio, R. and Blough, N. V.: Spatial and seasonal distribution of chromophoric dissolved organic  
453 matter and dissolved organic carbon in the Middle Atlantic Bight, in: *Marine Chemistry*, 169–187,  
454 <https://doi.org/10.1016/j.marchem.2004.02.027>, 2004.

455 Deutsch, B., Alling, V., Humborg, C., Korth, F., and Mörtz, C. M.: Tracing inputs of terrestrial high  
456 molecular weight dissolved organic matter within the Baltic Sea ecosystem, *Biogeosciences*, 9, 4465–4475,  
457 <https://doi.org/10.5194/bg-9-4465-2012>, 2012.

458 Dittmar, T., Lennartz, S. T., Buck-Wiese, H., Hansell, D. A., Santinelli, C., Vanni, C., Blasius, B., and  
459 Hehemann, J.-H.: Enigmatic persistence of dissolved organic matter in the ocean, *Nat Rev Earth Environ*, 2,  
460 570–583, <https://doi.org/10.1038/s43017-021-00183-7>, 2021.

461 DOSI: Ocean Alkalinity Enhancement Deep Ocean Stewardship Initiative Policy Brief, 2022.

462 Gattuso, J.-P., Mach, K. J., and Morgan, G.: Ocean acidification and its impacts: an expert survey, *Clim*  
463 *Change*, 117, 725–738, <https://doi.org/10.1007/s10584-012-0591-5>, 2013.

464 González, M. F. and Ilyina, T.: Impacts of artificial ocean alkalization on the carbon cycle and climate in  
465 Earth system simulations, *Geophys Res Lett*, 43, 6493–6502, <https://doi.org/10.1002/2016GL068576>, 2016.

466 Gore, S., Renforth, P., and Perkins, R.: The potential environmental response to increasing ocean alkalinity  
467 for negative emissions, *Mitig Adapt Strateg Glob Chang*, 24, 1191–1211, [https://doi.org/10.1007/s11027-](https://doi.org/10.1007/s11027-018-9830-z)  
468 018-9830-z, 2019.

469 Hansell, D., Carlson, C., Repeta, D., and Schlitzer, R.: Dissolved Organic Matter in the Ocean: A  
470 Controversy Stimulates New Insights, *Oceanography*, 22, 202–211,  
471 <https://doi.org/10.5670/oceanog.2009.109>, 2009.

472 Hansell, D. A.: Dissolved Organic Carbon Reference Material Program, *Eos, Transactions American*  
473 *Geophysical Union*, 86, 318, <https://doi.org/10.1029/2005EO350003>, 2005.

474 Heinze, C., Meyer, S., Goris, N., Anderson, L., Steinfeldt, R., Chang, N., Le Quéré, C., and Bakker, D. C. E.:  
475 The ocean carbon sink – impacts, vulnerabilities and challenges, *Earth System Dynamics*, 6, 327–358,  
476 <https://doi.org/10.5194/esd-6-327-2015>, 2015.

477 Helms, J. R., Stubbins, A., Ritchie, J. D., Minor, E. C., Kieber, D. J., and Mopper, K.: Absorption spectral  
478 slopes and slope ratios as indicators of molecular weight, source, and photobleaching of chromophoric  
479 dissolved organic matter, *Limnol Oceanogr*, 53, 955–969, <https://doi.org/10.4319/lo.2008.53.3.0955>, 2008.

480 Hinga, K.: Effects of pH on coastal marine phytoplankton, *Mar Ecol Prog Ser*, 238, 281–300,  
481 <https://doi.org/10.3354/meps238281>, 2002.

482 Hoikkala, L., Lahtinen, T., Perttilä, M., and Lignell, R.: Seasonal dynamics of dissolved organic matter on a  
483 coastal salinity gradient in the northern Baltic Sea, *Cont Shelf Res*, 45, 1–14,  
484 <https://doi.org/10.1016/j.csr.2012.04.008>, 2012.

485 Hoikkala, L., Kortelainen, P., Soinnie, H., and Kuosa, H.: Dissolved organic matter in the Baltic Sea, *Journal*  
486 *of Marine Systems*, 142, 47–61, <https://doi.org/10.1016/j.jmarsys.2014.10.005>, 2015.

487 Kaushal, N., Yang, L., Tanzil, J. T. I., Lee, J. N., Goodkin, N. F., and Martin, P.: Sub-annual fluorescence  
488 measurements of coral skeleton: relationship between skeletal luminescence and terrestrial humic-like  
489 substances, *Coral Reefs*, 39, 1257–1272, <https://doi.org/10.1007/s00338-020-01959-x>, 2020.

490 Kheshgi, H. S.: Sequestering atmospheric carbon dioxide by increasing ocean alkalinity, *Energy*, 20, 915–  
491 922, [https://doi.org/10.1016/0360-5442\(95\)00035-F](https://doi.org/10.1016/0360-5442(95)00035-F), 1995.

492 Kuliński, K., Schneider, B., Szymczycha, B., and Stokowski, M.: Structure and functioning of the acid–base  
493 system in the Baltic Sea, *Earth System Dynamics*, 8, 1107–1120, <https://doi.org/10.5194/esd-8-1107-2017>,  
494 2017.

- 495 Lawaetz, A. J. and Stedmon, C. A.: Fluorescence intensity calibration using the Raman scatter peak of water,  
496 *Appl Spectrosc*, 63, 936–940, <https://doi.org/10.1366/000370209788964548>, 2009.
- 497 Leenheer, J. A. and Reddy, M. M.:  $\text{CaCO}_3$ -precipitation of dissolved organic matter by calcium carbonate in  
498 pyramid lake, nevada, *Annals of Environmental Science*, 2008.
- 499 Moras, P., Menteş, T. O., Schiller, F., Ferrari, L., Topwal, D., Locatelli, A., Sheverdyayeva, P. M., and  
500 Carbone, C.: Reference plane for the electronic states in thin films on stepped surfaces, *Phys Rev B*, 103,  
501 165426, <https://doi.org/10.1103/PhysRevB.103.165426>, 2021.
- 502 Murphy, K. R., Stedmon, C. A., Graeber, D., and Bro, R.: Fluorescence spectroscopy and multi-way  
503 techniques. *PARAFAC, Analytical Methods*, 5, 6557, <https://doi.org/10.1039/c3ay41160e>, 2013.
- 504 Murphy, K. R., Stedmon, C. A., Wenig, P., and Bro, R.: OpenFluor- an online spectral library of auto-  
505 fluorescence by organic compounds in the environment, *Analytical Methods*, 6, 658–661,  
506 <https://doi.org/10.1039/C3AY41935E>, 2014.
- 507 Omanović, D., Santinelli, C., Marcinek, S., and Gonnelli, M.: ASFit - An all-inclusive tool for analysis of  
508 UV–Vis spectra of colored dissolved organic matter (CDOM), *Comput Geosci*, 133, 104334,  
509 <https://doi.org/10.1016/j.cageo.2019.104334>, 2019.
- 510 Omanović, D., Marcinek, S., and Santinelli, C.: TreatEEM—A Software Tool for the Interpretation of  
511 Fluorescence Excitation-Emission Matrices (EEMs) of Dissolved Organic Matter in Natural Waters, *Water*  
512 (Basel), 15, 2214, <https://doi.org/10.3390/w15122214>, 2023.
- 513 Pace, M. L., Reche, I., Cole, J. J., Fernández-Barbero, A., Mazuecos, I. P., and Prairie, Y. T.: pH change  
514 induces shifts in the size and light absorption of dissolved organic matter, *Biogeochemistry*, 108, 109–118,  
515 <https://doi.org/10.1007/s10533-011-9576-0>, 2012.
- 516 Royal Society and Royal Academy of Engineering: Greenhouse Gas Removal, 2018.
- 517 Santinelli, C.: DOC in the Mediterranean Sea, in: *Biogeochemistry of Marine Dissolved Organic Matter*,  
518 edited by: Hansell, D. A., Elsevier, 579–608, <https://doi.org/10.1016/B978-0-12-405940-5.00013-3>, 2015.
- 519 Santinelli, C., Nannicini, L., and Seritti, A.: DOC dynamics in the meso and bathypelagic layers of the  
520 Mediterranean Sea, *Deep Sea Research Part II: Topical Studies in Oceanography*, 57, 1446–1459,  
521 <https://doi.org/10.1016/j.dsr2.2010.02.014>, 2010.
- 522 Santinelli, C., Hansell, D. A., and Ribera d’Alcalà, M.: Influence of stratification on marine dissolved  
523 organic carbon (DOC) dynamics: The Mediterranean Sea case, *Prog Oceanogr*, 119, 68–77,  
524 <https://doi.org/10.1016/j.pocean.2013.06.001>, 2013.
- 525 Santinelli, C., Follett, C., Retelletti Brogi, S., Xu, L., and Repeta, D.: Carbon isotope measurements reveal  
526 unexpected cycling of dissolved organic matter in the deep Mediterranean Sea, *Mar Chem*, 177, 267–277,  
527 <https://doi.org/10.1016/j.marchem.2015.06.018>, 2015.
- 528 Seidel, M., Manecki, M., Herlemann, D. P. R., Deutsch, B., Schulz-Bull, D., Jürgens, K., and Dittmar, T.:  
529 Composition and Transformation of Dissolved Organic Matter in the Baltic Sea, *Front Earth Sci (Lausanne)*,  
530 5, <https://doi.org/10.3389/feart.2017.00031>, 2017.
- 531 Weishaar, J., Aiken, G., Bergamaschi, B., Fram, M., Fujii, R., and Mopper, K.: Evaluation of specific ultra-  
532 violet absorbance as an indicator of the chemical content of dissolved organic carbon, *Environ Sci Technol*,  
533 37, 4702–4708, <https://doi.org/10.1021/es030360x>, 2003.
- 534 Zigah, P. K., McNichol, A. P., Xu, L., Johnson, C., Santinelli, C., Karl, D. M., and Repeta, D. J.:  
535 Allochthonous sources and dynamic cycling of ocean dissolved organic carbon revealed by carbon isotopes,  
536 *Geophys Res Lett*, 44, 2407–2415, <https://doi.org/10.1002/2016GL071348>, 2017.

537